Rotation Measure studies of the quasar 3C 345 with RadioAstron

University College Cork, Ireland
Coláiste na hOllscoile Corcaigh

F. M. Pötzl[1,2], on behalf of the RadioAstron KSP on AGN Polarization

1 - Physics Department, University College Cork, Ireland   2 - Max-Planck-Institut für Radioastronomie, Bonn, Germany

Max-Planck-Institut für Radioastronomie

The RadioAstron Polarization KSP

Supermassive black holes in the centres of radio-loud active galactic nuclei (AGN) produce collimated relativistic outflows (jets). Space-VLBI observations within the RadioAstron (Kardashev et al. 2013) key science program on AGN polarization provide images at an unprecedented resolution, which enables us to study the magnetic field strength and morphology in the innermost regions of AGN jets. 11 of the brightest and highly polarised AGN were observed during observing periods AO-1, -2, -3, -4 and -5 between July 2013 and April 2018, where operations of the spacecraft ceased in 2019 (Pashchenko et al. 2015; Lobanov et al. 2015; Gómez et al. 2016; Bruni et al. 2017; Kravchenko et al. 2020; Pötzl et al. 2021; Savolainen et al. 2021; Gómez et al. 2022).

Magnetic fields in AGN

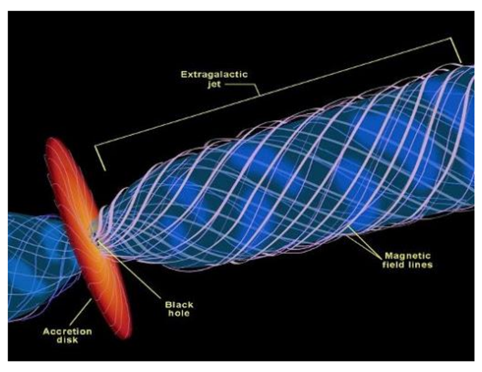

Many theoretical models of jet launching predict a helical magnetic field (e.g., Meier et al. 2011, Zamaninasab et al. 2014). Testing the 3D-structure of the B-field in AGN sheds light on the nature of jet launching and collimation. The line-of-sight component can be studied with Faraday rotation, where the Electric Vector Position Angles (EVPAs) are rotated as a function of wavelength, with RM denoting the Rotation Measure.

$$\Delta\chi = RM \cdot \lambda^2 \propto \int_s n_e B_{\parallel} ds \cdot \lambda^2$$

Recent studies on a large sample of AGN have shown a tendency for EVPAs to be aligned with the jet in BL Lac objects, with quasars having less of that tendency (Pushkarev et al. 2017).

Observations

Observations of the quasar 3C 345 (e.g., Ros et al. 2000, Schinzel et al. 2012) (z = 0.59) at λ = 18 cm took place on March 30 & March 31 2016 during AO-3, and with a total of eighteen antennas from a ground array (VLBA+EVN) were observing, complemented by the *Spekt-R* space telescope. We detect ground-space fringes up to **9 earth diameters** (for details, see Pötzl et al. 2021). Here we use complementary VLBA data at 4.8, 8.4 and 15.3 GHz from the same or nearby epoch.

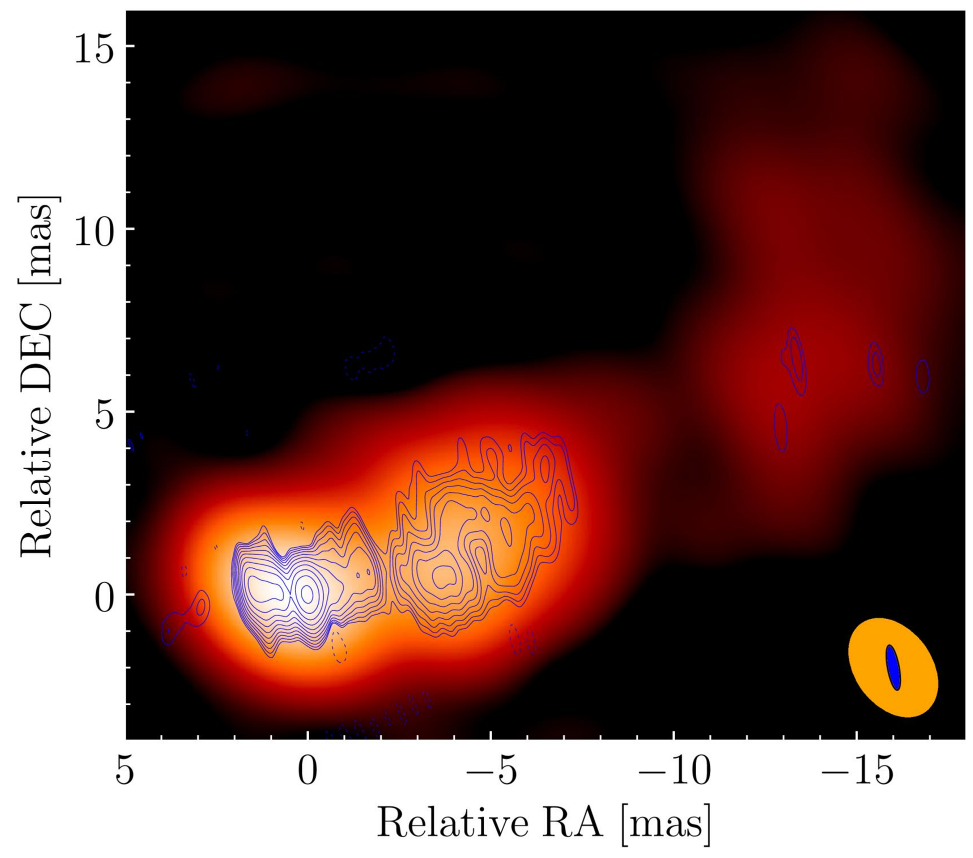

Left: 3C 345 at 1.6 GHz with RadioAstron, overlaid as contours over the ground array image obtained from the same observation. The respective synthesized beams of the two images are shown in the lower right corner. The beam minor axis is 2.326 mas (15.6 pc) for the ground array, and 0.283 mas (1.9 pc) with RadioAstron. We used a uniform weighting scheme.

Map alignment

We aligned images at several frequencies by convolving them with the 8.4 GHz restoring beam (slightly over-resolving the 4.8 GHz map) and using the smallest pixel size, and then using a 2D-cross correlation algorithm (Baczko, in prep.) to find the positional shift.

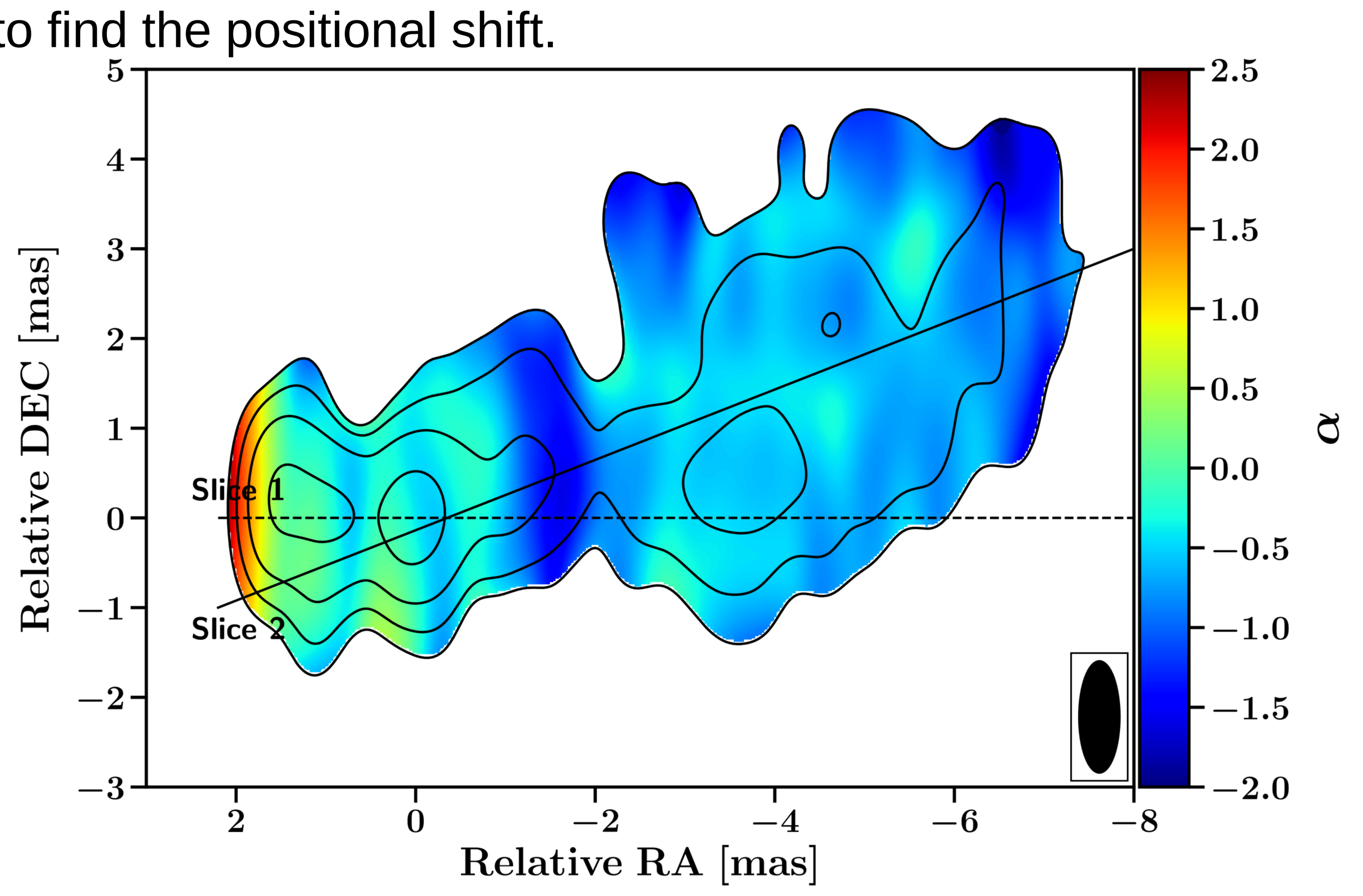

Top: Spectral index map ($S_\nu \propto \nu^\alpha$) between the 1.6 GHz RadioAstron and 15 GHz MOJAVE (Lister et al. 2018) image. The optically thick core and the region of increased opacity close to the emission peak are clearly visible, indicating a shock travelling down the jet.

Results

After subtracting galactic foreground RM, we tried to fit all four frequencies for rotation measure, using the error analysis presented in Hovatta et al. (2012), and allowing for several $n\pi$-rotations. However, the regions with significant polarised intensity differ dramatically over the studied frequency range, yielding poor fits. Hence, we fitted the upper and lower three frequencies, and obtained good results for the RM map between 1.6 and 8.4 GHz.

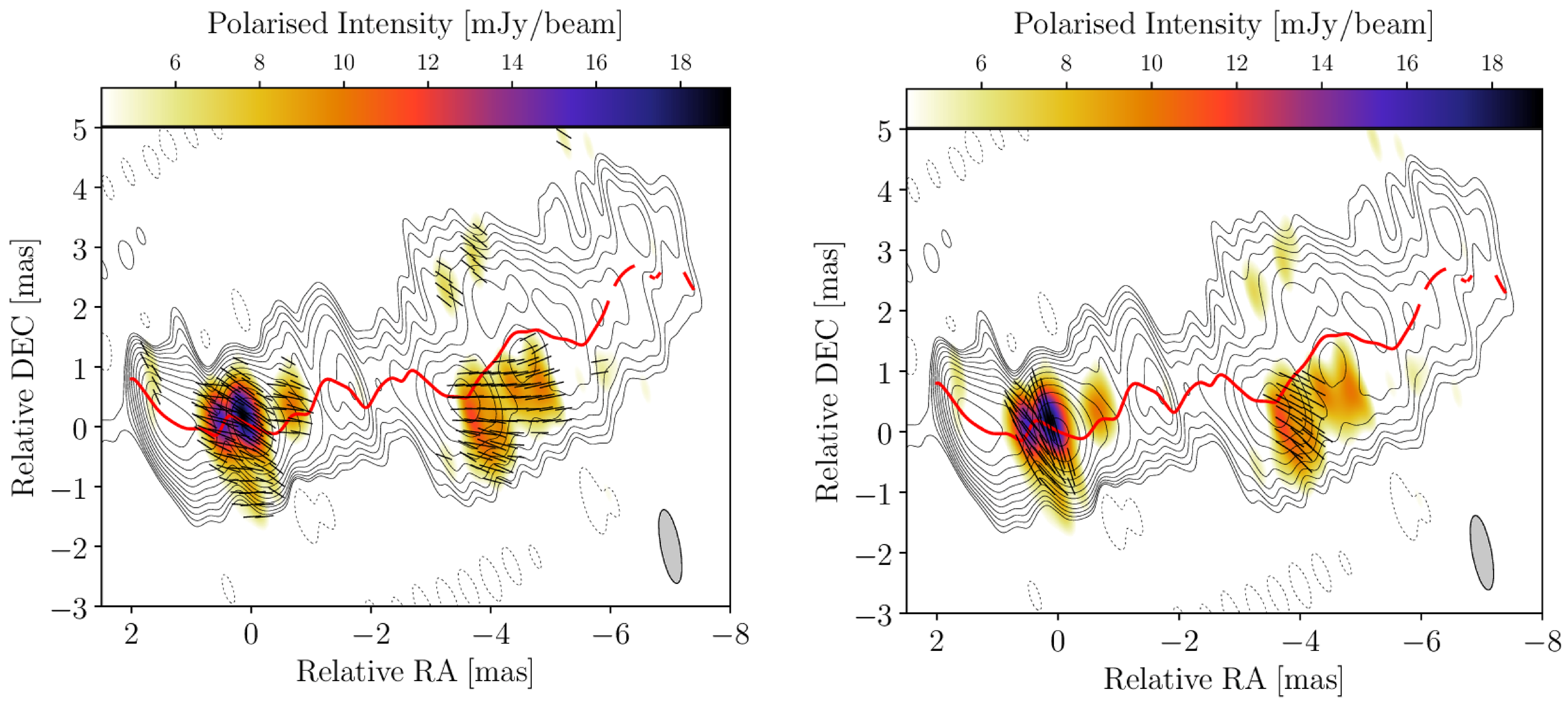

Top left: 1.6 GHz linear polarisation map with EVPAs seemingly aligned with the local jet direction (indicated by the jet ridge line in red), uncorrected for RM. The fractional polarisation at the peak brightness location is about 5 %. *Top right*: Same map with EVPAs corrected, where significant RM fits have been calculated.

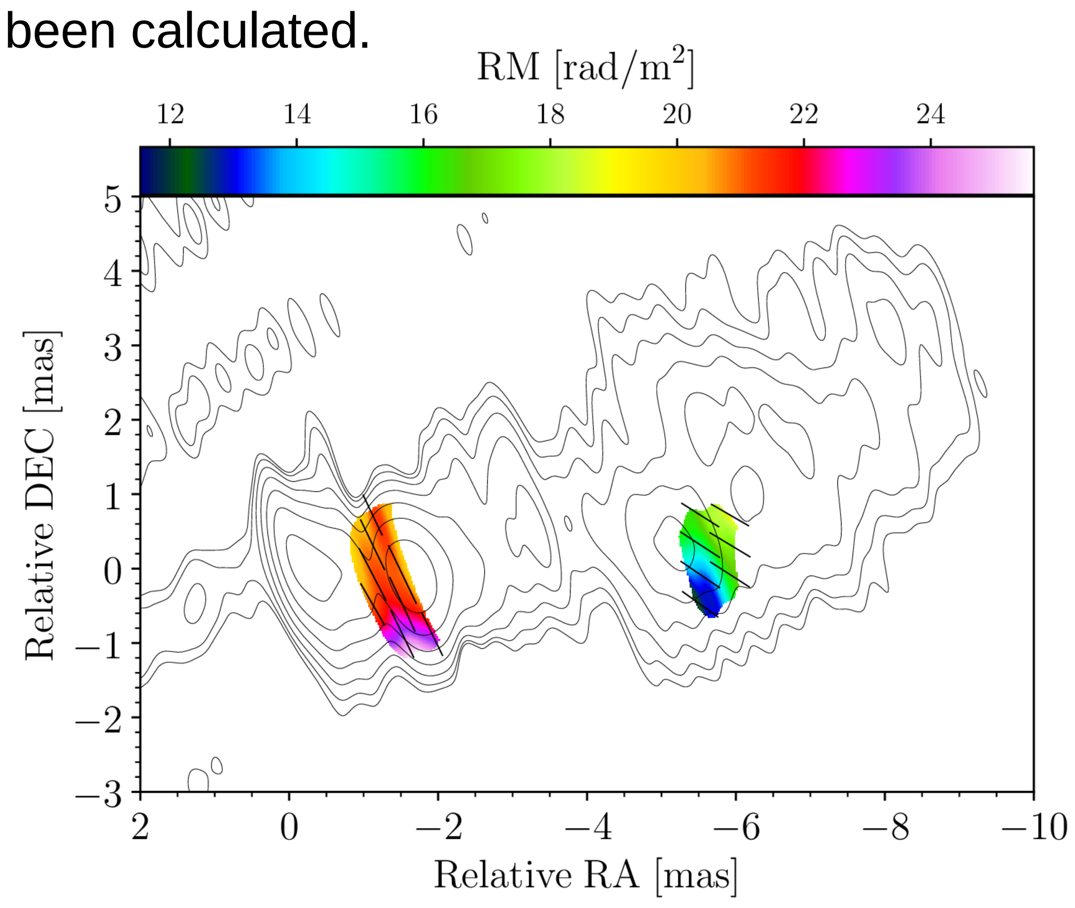

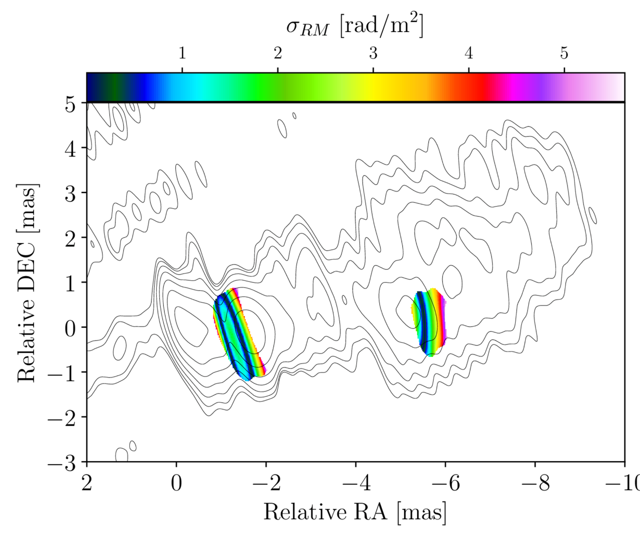

Left (top): RM(-error) map obtained from 1.6, 4.8 and 8.4 GHz polmap. There is an indication of a transverse RM gradient, hinting at a toroidal B-field, but it is not yet detected with significance.

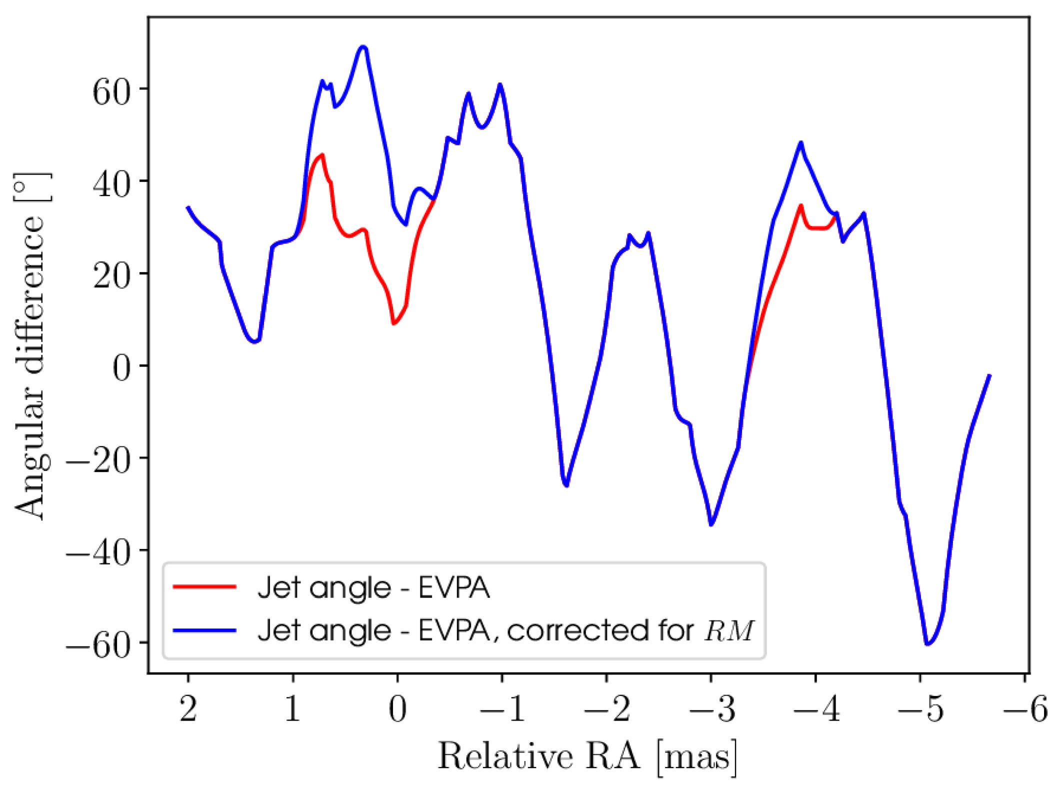

Left: Difference of jet local jet direction (calculated as moving average) and EVPAs, with and without RM-correction. At the brightness peak location, there might be a change from EVPAs aligned with the jet to being rather perpendicular.

Conclusions & Outlook

RadioAstron allows us to study the polarisation properties of AGN at unprecedented resolution at low radio frequencies. Combined with ground-array observations at higher frequencies, it even allows the study of rotation measure at ultra-high resolution. Our findings for the quasar 3C 345 suggest that Faraday rotation may significantly change the orientation of EVPAs with respect to the direction of the parsec-scale jet, indicating more a poloidal than a toroidal B-field. The connection with shocks in the jet plasma may still be valid, in the sense that the magnetic field uniformity is enhanced by compression. However, this needs further investigation (feedback appreciated!). We see a possible transverse gradient in RM in the jet, indicating also a toroidal B-field, that might be part of a helical one, as has already been shown to exist in many AGN jets at lower resolution (e.g., Motter & Gabuzda 2017, also for 3C 345). We are looking to study more epochs to investigate the evolution of EVPAs and RM with time.

References

Bruni, G. et al. 2017, A&A 604, A111; Goméz, J. L. et al. 2016, ApJ 817, 96; Goméz, J. L. et al. 2022, ApJ 924, 122; Hovatta, T. et al. 2012, AJ 144, 105; Kardashev, N. S. et al. 2013, Astron. Rep. 57, 153; Kravchenko, E. V. et al. 2020, ApJ, 893, 68; Lister, M. L. et al. 2018, ApJS 232, 12; Lobanov, A. P. 2015, A&A 574, A84; Meier, D. L. et al. 2001, Science 291, 84; Motter, J. C. & Gabuzda, D. C. 2017, MNRAS 467, 2648; Pötzl et al. 2021, A&A 648, A82; Pushkarev, A. et al. 2017, Galaxies 5, 93; Ros, E. et al. 2000, A&A 354, 55; Savolainen, T. et al. 2021, arXiv:2111.04481, submitted to A&A; Schinzel, F. et al. 2012, A&A, 537, 70; Zamaninasab, M. et al. 2014, Nature 510, 126;